

This article was downloaded by:

On: 14 January 2011

Access details: *Access Details: Free Access*

Publisher *Taylor & Francis*

Informa Ltd Registered in England and Wales Registered Number: 1072954 Registered office: Mortimer House, 37-41 Mortimer Street, London W1T 3JH, UK



Molecular Simulation

Publication details, including instructions for authors and subscription information:

<http://www.informaworld.com/smpp/title~content=t713644482>

Molecular dynamics simulation of time-irreversibility of stationary heat flux

Toshiki Mima^{ab}; Kenji Yasuoka^b; Shuichi Nosé^a

^a Department of Physics, Keio University, Keio, Japan ^b Department of Mechanical Engineering, Keio University, Keio, Japan

To cite this Article Mima, Toshiki, Yasuoka, Kenji and Nosé, Shuichi (2007) 'Molecular dynamics simulation of time-irreversibility of stationary heat flux', *Molecular Simulation*, 33: 1, 109 – 113

To link to this Article: DOI: 10.1080/08927020601067565

URL: <http://dx.doi.org/10.1080/08927020601067565>

PLEASE SCROLL DOWN FOR ARTICLE

Full terms and conditions of use: <http://www.informaworld.com/terms-and-conditions-of-access.pdf>

This article may be used for research, teaching and private study purposes. Any substantial or systematic reproduction, re-distribution, re-selling, loan or sub-licensing, systematic supply or distribution in any form to anyone is expressly forbidden.

The publisher does not give any warranty express or implied or make any representation that the contents will be complete or accurate or up to date. The accuracy of any instructions, formulae and drug doses should be independently verified with primary sources. The publisher shall not be liable for any loss, actions, claims, proceedings, demand or costs or damages whatsoever or howsoever caused arising directly or indirectly in connection with or arising out of the use of this material.

Molecular dynamics simulation of time-irreversibility of stationary heat flux

TOSHIKI MIMA^{†‡*}, KENJI YASUOKA[‡] and SHUICHI NOSÉ^{†¶}

[†]Department of Physics, Keio University, Keio, Japan

[‡]Department of Mechanical Engineering, Keio University, Keio, Japan

(Received 17 September 2006; in final form 16 October 2006)

Molecular dynamics simulations are carried out to monitor heat flux directly, in both forward process and time-reversed process. Two weighted Nosé–Hoover thermostats, whose temperatures are different independently, are attached to a Stillinger–Weber fcc crystal confined by reflective walls. With increasing temperature difference, phase-space collapse rate in the forward process decreased and the irreversibility of heat flux appeared earlier in time-reversed process. The irreversibility appeared earlier, with decreasing numbers of significant digits. Nevertheless, the values of phase-space collapse rate were almost same.

Keywords: Time reversibility; Chaos; Nonequilibrium state; Heat conduction; Molecular dynamics simulation; Nosé–Hoover thermostat

1. Introduction

Hoover proposed a theory that explains the origin of Clausius's principle, the second law of thermodynamics, on the basis of mechanics [1]. On the theory, first, it is imposed that numbers of significant digits of physical quantities are finite, even in classical mechanics due to the uncertainty principle of quantum mechanics. Then contraction of information continuously occurs in the forward process that a stationary heat flux flows from high temperature part to low temperature part. Thus when the direction of the heat flux is reversed in the case of the time-reversed process, the deviation from the forward process grows exponentially, and the time-irreversibility appears in a finite time. Finally time-reversed process is unstable and cannot be observed.

For example, we can consider a system which is partially connected to a high temperature thermostat and a low temperature thermostat; two thermostats are connected to the same number of particles, N , individually and are controlled by Nosé–Hoover method. The variables of the system are $\Gamma = (\mathbf{q}_1, \dots, \mathbf{q}_{N_s}, \mathbf{p}_1, \dots, \mathbf{p}_{N_s}, \zeta_{\text{high}}, \zeta_{\text{low}})$ where N_s is the number of all particles, q_i is the position of i -th particle, p_i is the momentum of i -th particles, ζ_{high} is the friction variable of thermostat of high temperature,

T_{high} , and ζ_{low} is the friction variable of thermostat of low temperature, T_{low} . The time evolution of the distribution function f in stationary state is derived by Liouville equation:

$$\frac{\partial f}{\partial t} = - \left[\frac{\partial}{\partial \mathbf{q}} + \frac{\partial}{\partial \mathbf{p}} + \frac{\partial}{\partial \zeta_{\text{high}}} + \frac{\partial}{\partial \zeta_{\text{low}}} \right] (\Gamma f) \Rightarrow \frac{df}{dt} = 3N(\langle \zeta_{\text{high}} \rangle + \langle \zeta_{\text{low}} \rangle) f \quad (1)$$

$$\Rightarrow f(\Gamma(t)) = f(\Gamma(0)) \exp[3N(\langle \zeta_{\text{high}} \rangle + \langle \zeta_{\text{low}} \rangle)t]. \quad (2)$$

Considering the balance of heat in the forward process, that is, $3N\langle \zeta_{\text{low}} \rangle T_{\text{low}} + 3N\langle \zeta_{\text{high}} \rangle T_{\text{high}} = 0$ and $\langle \zeta_{\text{low}} \rangle > 0$, the equation (2) can be written in terms of the two temperatures:

$$\Rightarrow f(\Gamma(t)) = f(\Gamma(0)) \exp \left[3N\langle \zeta_{\text{low}} \rangle \left(1 - \frac{T_{\text{low}}}{T_{\text{high}}} \right) t \right], \rightarrow +\infty \quad (3)$$

Because the integration of f over whole phase space is unity, the phase-space volume element collapses to zero and the information contracts continuously in the forward process. The negative value of the exponent, $3N\langle \zeta_{\text{low}} \rangle (1 - T_{\text{low}}/T_{\text{high}})$, can be defined as the collapse rate of phase-space volume element and the product of the

*Corresponding author. Email: t_mima@z8.keio.jp

¶Deceased.

exponent by Boltzmann constant can be defined as the entropy production rate. Such trajectories go to attractors and they are stable. On the other hand, phase-space volume element diverges in time-reversed process. In this situation trajectories go from repellers and they are unstable. Hoover *et al.* have researched various kinds of nonequilibrium systems [2–6]. However the heat flux in both forward and time-reversed processes have not been monitored directly.

In this paper, the irreversibility of heat flux is monitored directly on the basis of the above theory. First, the system of the interest and the equations of motion are introduced in section 2. Then the behavior of heat flux in both forward and time-reversed processes are showed and the effects on heat flux by temperature difference and numbers of significant digits are investigated in section 3.

2. Method

Figure 1 shows the system of interest. A total of 16,000 particles interacting with Stillinger–Weber potential [7]

$$\phi(r_{ij}) = \begin{cases} a_{\text{SW}} \left[\frac{1}{r_{ij}^{12}} - 1 \right] \exp \left[\frac{1}{r_{\text{SW}} - r_{ij}} \right] & (0 < r_{ij} < r_{\text{SW}}) \\ 0 & (\text{otherwise}), \end{cases} \quad (4)$$

$$a_{\text{SW}} = 8.805977, \quad r_{\text{SW}} = 1.652194.$$

took fcc lattice. a_{SW} and r_{SW} are set to coincide Lennard–Jones repulsive core, therefore, this fcc crystal is stable. Stillinger–Weber potential does not cause any cutoff error. The crystal was confined in the rectangular cell with reflective walls whose size was $(L_x, L_y, L_z) = (15.62, 15.62, 62.47)$, namely, the uniform number density is 1.05. The particles in the region $0 \leq z < 0.25L_z$ were

attached to the high temperature thermostat and the particles in the region $0.75L_z \leq z < L_z$ were attached to the low temperature thermostat. The heat flux, therefore, is positive in normal stationary state: time-reversed process. Two thermostats were weighted Nosé–Hoover type [8]. The equations of motion of temperature-controlled particles were defined as follows:

$$\begin{aligned} \frac{d\mathbf{q}_i}{dt} &= \frac{\mathbf{p}_i}{m}, \quad \frac{d\mathbf{p}_i}{dt} = -\frac{\partial \phi}{\partial \mathbf{q}_i} - w_{\#}(z_i) \zeta_{\#} \mathbf{p}_i, \\ \frac{d\zeta_{\#}}{dt} &= \frac{1}{Q_{\#}} \sum_{i \in C_{\#}} \left[\frac{p_i^2}{m} - 3w_{\#}(z_i) k_B T_{\#} \right], \end{aligned} \quad (5)$$

where # stands for “low” or “high”, and smooth weighting functions $w_{\#}$ are defined so as not to make error in changing equations of motion near $z = 0.25L_z$ and $z = 0.75L_z$,

$$w_{\text{high}}(z_i) = \begin{cases} 1 & (z_i < 0.2L_z) \\ 0.5 \left(1 + \cos \pi \left(\frac{z_i - 0.2L_z}{0.05L_z} \right) \right) & (0.2L_z \leq z_i < 0.25L_z) \\ 0 & (z_i \geq 0.25L_z) \end{cases} \quad (6)$$

$$w_{\text{low}}(z_i) = \begin{cases} 0 & (z_i < 0.75L_z) \\ 0.5 \left(1 - \cos \pi \left(\frac{z_i - 0.75L_z}{0.05L_z} \right) \right) & (0.75L_z \leq z_i < 0.8L_z) \\ 1 & (z_i \geq 0.8L_z) \end{cases} \quad (7)$$

The particles in $0.25L_z \leq z_i < 0.75L_z$ obeyed simple Newton’s equations of motion. In this case, the time evolution of

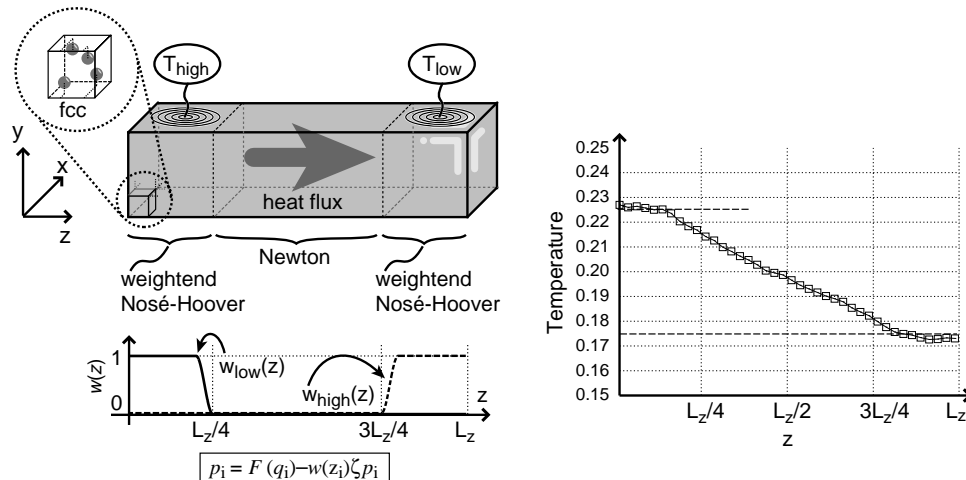


Figure 1. Left: schematic figure of system. The heat flux j_z is positive in the forward process and weight functions for two thermostats. Right: temperature profile. $T_{\text{high}} = 0.225$, $T_{\text{low}} = 0.175$. Local temperatures are calculated by $T_i = (2/3N_i) \sum_{j \in C_i} \mathbf{p}_j^2 / 2m$ where C_i is the i -th part of simulation box and N_i is the number of particles in C_i .

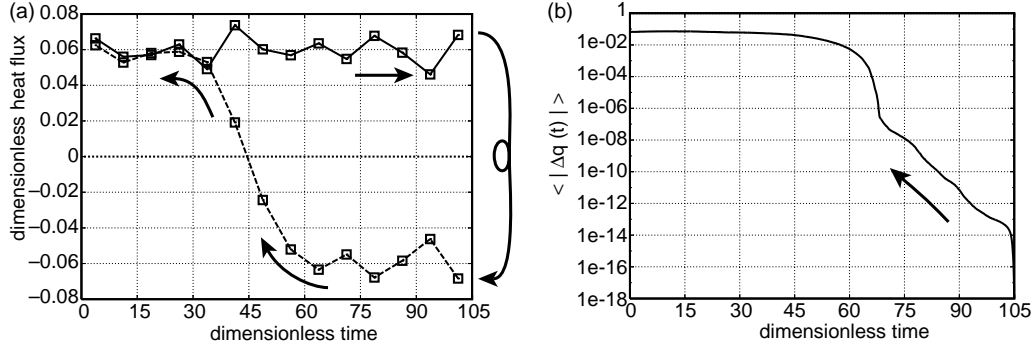


Figure 2. An example of monitoring. $T_{\text{high}} = 0.125$, $T_{\text{low}} = 0.075$. Left: monitoring heat flux in both forward and time-reversed processes, Right: monitoring $\langle |\Delta q(t)| \rangle$ in time-reversed process corresponding to the left part.

the distribution function is

$$f(\mathbf{\Gamma}(t)) = f(\mathbf{\Gamma}(0)) \exp \left[3 \left\langle \left(\sum_{i \in C_{\text{high}}} w_{\text{high}}(z_i) \right) \zeta_{\text{high}} \right\rangle + 3 \left\langle \left(\sum_{i \in C_{\text{low}}} w_{\text{low}}(z_i) \right) \zeta_{\text{low}} \right\rangle \right] t, \quad (8)$$

considering the balance of heat again, $3 \langle \sum_{i \in C_{\text{low}}} w_{\text{low}} \zeta_{\text{low}} \rangle T_{\text{low}} + 3 \langle \sum_{i \in C_{\text{high}}} w_{\text{high}} \zeta_{\text{high}} \rangle T_{\text{high}} = 0$,

$$= f(\mathbf{\Gamma}(0)) \exp \left[3 \left\langle \left(\sum_{i \in C_{\text{low}}} w_{\text{low}}(z_i) \right) \zeta_{\text{low}} \right\rangle \left(1 - \frac{T_{\text{low}}}{T_{\text{high}}} \right) t \right]. \quad (9)$$

In all simulations m was unity. We chose the value of mass of thermostat $Q_{\#}$ from unity to seven according to the temperature of the thermostat. All equations of motion were integrated numerically on the basis of a time-reversible Leap-Frog algorithm. The time step was set to 0.005 in all simulations. Variables with double precision were used. The heat flux component j_z was calculated

from particles in the region $0.25L_z < z < 0.75L_z$,

$$j_z = \frac{1}{V} \sum_{i \in C_j} \left[\varepsilon_i \frac{p_{iz}}{m} - \left(\frac{1}{2} \sum_{j \neq i} (q_{zi} - q_{zj}) \frac{\partial \phi}{\partial \mathbf{q}_i} \right) \cdot \frac{\mathbf{p}_i}{m} \right], \quad (10)$$

$$\varepsilon_i = \frac{\mathbf{p}_i^2}{2m} + \frac{1}{2} \sum_{j \neq i} \phi(|\mathbf{q}_i - \mathbf{q}_j|).$$

The simulation has three processes. First, the crystal with temperature difference was prepared without particular rescalings and corrections: the positive stationary heat flux arose in this forward process. Then physical quantities were monitored for 21,000 steps. Then, the signs of all momenta and friction variables were reversed,

$$\mathbf{p}_i \rightarrow -\mathbf{p}_i (1 \leq i \leq N), \quad \zeta_{\text{low}} \rightarrow -\zeta_{\text{high}}, \quad \zeta_{\text{high}} \rightarrow -\zeta_{\text{low}},$$

and physical quantities were monitored in time-reversed process.

Table 1. Uniform temperature, temperature difference and the phase-space collapse rate. The phase-space collapse rate at four points of temperature difference are calculated at each uniform temperature.

		ΔT					
		0.025	0.050	0.075	0.100	0.150	0.200
T_{uni}	0.1	-18.2 ± 8.9	-76.4 ± 9.5	-187.3 ± 9.6	-379.7 ± 10.2	—	—
	0.2	—	-11.5 ± 8.3	—	-52.8 ± 8.9	-128.2 ± 9.1	-262.5 ± 8.8
	0.3	—	-7.1 ± 8.6	—	-17.1 ± 9.3	-39.7 ± 8.8	-75.4 ± 9.4

Table 2. Uniform temperature, temperature difference and the time of irreversibility. The times of irreversibility at four points of temperature difference are calculated at each uniform temperature.

		ΔT					
		0.025	0.050	0.075	0.100	0.150	0.200
T_{uni}	0.1	63.7 ± 1.0	62.8 ± 1.4	61.6 ± 1.3	54.4 ± 1.4	—	—
	0.2	—	42.8 ± 0.8	—	41.6 ± 1.1	37.1 ± 0.7	35.8 ± 0.6
	0.3	—	29.8 ± 1.0	—	29.8 ± 0.2	28.2 ± 0.5	27.7 ± 0.2

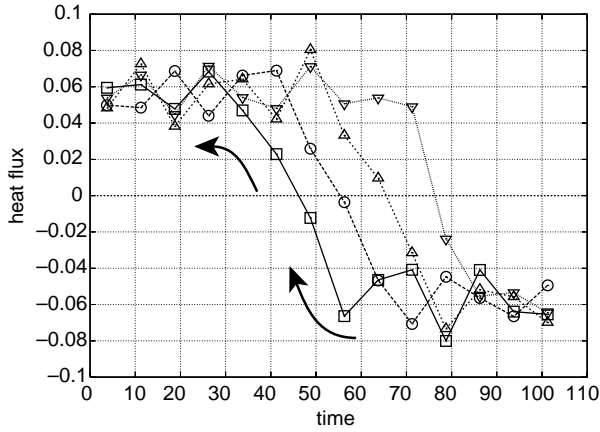


Figure 3. Monitoring of heat fluxes in time-reversed process as the function of numbers of significant digits. Numbers of significant digits are 10^{-7} (solid line), 10^{-8} (dashed line), 10^{-11} (dotted line) and 10^{-13} (solid-dotted line).

3. Result

The left part of figure 2 shows a general behavior of stationary heat fluxes in both forward and time-reversed process. In the forward process, heat flux was stable and takes a nearly constant positive value. On the other hand, the sign of the heat flux in time-reversed process was negative temporarily and the shape looked like the mirror image of the heat flux in the forward process. However, the sign suddenly turned to positive as the error of time-reversed process against the forward process were accumulating. Such behavior was monitored over all simulations. To investigate irreversibility from the point of view of accumulation of microscopic error, the average of deviation of time-reversed particles' trajectories against the forward trajectories, $\langle \delta q(t) \rangle$, were calculated:

$$\langle |\delta q(t)| \rangle = \frac{1}{N} \sum_{i=1}^N |q(t)_{\text{rev}} - q(t)_{\text{pro}}|. \quad (11)$$

The right part of figure 2 shows $\langle \delta q(t) \rangle$ monitored in time-reversed process corresponding to the left part of the figure. $\langle \delta q(t) \rangle$ increased exponentially as soon as time-reversed process begins, however, net deviation is so small that the sign of heat flux is still negative. This increase stopped when the order of $\langle \delta q(t) \rangle$ became 0.1, then, the sign of the heat flux turned to positive. This figure shows Lyapunov instability of time-reversed process directly. This result shows that the irreversibility appears on heat

flux when the order of $\langle \delta q(t) \rangle$ is equal to the order of the amplitude of the lattice vibration.

On the basis of the equation (8), the relation between temperature difference $\Delta T = T_{\text{high}} - T_{\text{low}}$ and irreversibility of heat flux were investigated. For convenience, we defined uniform temperature, $T_{\text{uni}} = (T_{\text{low}} + T_{\text{high}})/2$, and the period from the time when time-reversed process began to the time when heat flux crosses $j_z = 0$, τ . Table 1 shows the relation between temperature difference ΔT and phase-space collapse rate, $-3\langle (\sum_{i \in C_{\text{high}}} w_{\text{high}}(z_i)) \zeta_{\text{high}} \rangle - 3\langle (\sum_{i \in C_{\text{low}}} w_{\text{low}}(z_i)) \zeta_{\text{low}} \rangle$, as the function of T_{uni} and table 2 shows the relation between temperature difference ΔT and τ as the function of T_{uni} . Simulations were carried out for four values of ΔT every T_{uni} . Average values and their errors were calculated over ten samples. With increasing ΔT , the phase-space collapse rates decreased, τ decreased and irreversibility of heat flux appeared early. It is found that the phase-space collapse rate decreases monotonically and τ decreases when the magnitude of nonequilibrium increases if two masses of thermostats have suitable values for the crystal.

Imposing finiteness on numbers of significant digits of physical quantities, Hoover has developed irreversibility of heat-conducting system. To investigate relation between irreversibility and the numbers of significant digits, four kinds of artificial round-off errors were added every timestep to variables in phase-space whose absolute value were 10^{-8} , 10^{-10} , 10^{-12} and 10^{-14} individually; numbers of significant digits are 7, 9, 11 and 13 correspondingly. Figure 3 shows four kinds of heat flux in time-reversed process. The smaller numbers of significant digits, the smaller τ and there was a linear relation. Four phase-space collapse rates, however, equaled over all numbers of significant digits (table 3). This result means $\langle |\delta q(t)| \rangle$ accumulates error of the order of artificial round-off error right after time-reversed then grows with the same exponents.

4. Conclusion

We have studied molecular dynamics simulation on nonequilibrium stationary heat flux, conducting in Stillinger–Weber crystal on the Hoover's theory. Irreversibility of heat flux in time-reversed process appeared when the deviation of a particle's trajectory against one in the forward process grew to the order of lattice vibration. Because phase-space collapse rate increased in the forward process with increasing temperature difference, time at which irreversibility of heat flux appears in time-

Table 3. Numbers of significant digits and phase-space collapse rates. $T_{\text{uni}} = 0.1$, $\Delta T = 0.05$.

Numbers of significant digits	7	9	11	13
Entropy production	-76.6 ± 1.9	-74.2 ± 1.5	-75.4 ± 1.5	-74.7 ± 0.7
τ	29.8 ± 0.8	39.3 ± 2.0	53.4 ± 2.4	58.0 ± 2.8

reversed process decreased. Numbers of significant digits had no relation to the value of heat flux in stationary state, The value of heat flux in stationary state did not depend on numbers of significant digits, on the other hand, the time at which irreversibility of heat flux appeared decreases linearly with decreasing of them.

Acknowledgements

The authors appreciate W. Hoover for checking the draft and helpful discussion on time-reversibility. This work is supported by Grant in Aid for the 21st C.O.E. program at Keio University for “System Design: Paradigm Shift from Intelligence to Life”.

References

- [1] B.L. Holian, W.G. Hoover, A. Posch. Resolution of loschmidt's paradox: the origin of irreversible behavior in reversible atomistic dynamics. *Phys. Rev. Lett.*, **59**, 10 (1987).
- [2] W.G. Hoover. *Time Reversibility, Computer Simulation, and Chaos*, World Scientific Publishing, Singapore (1999).
- [3] H.A. Posch, G. Hoover. Lyapunov instability of dense Lennard-Jones fluids. *Phys. Rev. A*, **38**, 473 (1988).
- [4] W.G. Hoover. Reversible mechanics and time's arrow. *Phys. Rev. A*, **37**, 252 (1988).
- [5] H.A. Posch, G. Hoover. Large-system phase-space dimensionality loss in stationary heat flows. *Physica D*, **187**, 281 (2004).
- [6] H.A. Posch, G. Hoover. Time-reversible dissipative attractors in three and four phase-space dimensions. *Phys. Rev. E*, **55**, 6803 (1997).
- [7] F.H. Stillinger, A. Weber. Inherent pair correlation in simple liquids. *J. Chem. Phys.*, **80**, 4434 (1984).
- [8] S. Nosé. Constant temperature molecular dynamics methods. *Prog. Theor. Phys. Suppl.*, **103**, 1 (1991).